

# The TTF finite-energy spectral features in photoemission of TTF-TCNQ: The Hubbard-chain description

D. Bozi<sup>1</sup>, J. M. P. Carmelo<sup>2</sup>, K. Penc<sup>3</sup>, P. D. Sacramento<sup>4</sup>

<sup>1</sup>Centro de Física de Materiales, Centro Mixto CSIC-UPV/EHU, E-20018 San Sebastian, Spain

<sup>2</sup>GCEP-Center of Physics, U. Minho, Campus Gualtar, P-4710-057 Braga, Portugal

<sup>3</sup>Res. Inst. for Solid State Physics and Optics, H-1525 Budapest, P.O.B. 49, Hungary

<sup>4</sup>Departamento de Física and CFIF, IST, Universidade Técnica de Lisboa, Av.

Rovisco Pais, 1049-001 Lisboa, Portugal

E-mail: carmelo@fisica.uminho.pt

**Abstract.** A dynamical theory which accounts for all microscopic one-electron processes is used to study the spectral function of the 1D Hubbard model for the whole  $(k, \omega)$ -plane, beyond previous studies which focused on the weight distribution in the vicinity of the singular branch lines only. While our predictions agree with those of the latter studies concerning the tetracyanoquinodimethane (TCNQ) related singular features in photoemission of the organic compound tetrathiafulvalene-tetracyanoquinodimethane (TTF-TCNQ) metallic phase, the generalized theory also leads to quantitative agreement concerning the tetrathiafulvalene (TTF) related finite-energy spectral features, which are found to correspond to a value of the on-site repulsion  $U$  larger than for TCNQ. Our study reveals the microscopic mechanisms behind the unusual spectral features of TTF-TCNQ and provides a good overall description of those features for the whole  $(k, \omega)$ -plane.

PACS numbers: 71.10.Pm, 71.27.+a

Most early studies of quasi-one-dimensional (1D) conductors such as tetrathiafulvalene-tetracyanoquinodimethane (TTF-TCNQ) have focused on the various low-energy phases, which are not metallic and correspond to broken-symmetry states [1]. Recently, the resolution of photoemission experiments has improved, and the *normal* state of these compounds was found to display exotic spectral properties [2, 3, 4]. However, such a metallic state refers to finite energies and thus is not described by the usual low-energy schemes. Based on a new quantum-object description of the 1D Hubbard model [5], a preliminary version of the finite-energy dynamical theory considered here was used in the studies of Ref. [6], which provided the weight distribution in the vicinity of well-defined branch lines only. Those lines refer to theoretical singular spectral features, which were found to describe the sharpest TCNQ related spectral dispersions observed in TTF-TCNQ by angle-resolved photoelectron spectroscopy (ARPES). Further details of such preliminary studies on the sharpest TCNQ related spectral features are provided in Ref. [7]. In the mean while, a complete and more powerful version of the pseudofermion dynamical theory, which accounts for all one-electron microscopic processes, was presented in Refs. [8, 9]. (Such a general finite-energy theory recovers the known low-energy results in the limit of low energy, as confirmed in Ref. [10].)

In this paper the latter theory is suitably used to evaluate the momentum and energy dependence of the one-electron weight distribution of the model for the whole  $(k, \omega)$ -plane. While both our predictions and those of Ref. [11] (which refer to the TCNQ features only) agree with those of Ref. [6] for the TCNQ related singular features, we are also able to derive a theoretical weight distribution for the TTF related spectral features. For TTF the best quantitative agreement between the theory and experiments is reached for values of  $U$  larger than those preliminarily estimated in Ref. [6] for the TTF stack of molecules [12]. The  $U$  value found here for TTF is larger than for TCNQ, in agreement with results from the low-energy broken-symmetry phase [1]. Our study clarifies the microscopic processes behind the unusual spectral properties of TTF-TCNQ and provides a good overall description of its spectral features for the whole  $(k, \omega)$ -plane. It also reveals that the electronic degrees of freedom of the *normal* state of quasi-1D metals reorganize for all energies in terms of charge and spin objects, whose scattering determines the unusual spectral properties.

The structure of the quasi-1D conductor TTF-TCNQ consists of parallel linear stacks of planar TTF and TCNQ molecules [1, 2, 4]. Its partial charge transfer is 0.59 electrons from the donor (TTF) to the acceptor (TCNQ) and thus the electronic densities are  $n = 1.41$  and  $n = 0.59$ , respectively. Due to electronic correlations, the optical properties of the metallic phase depart significantly from Drude-free-electron behavior [1] and the finite-energy electronic structure, as probed by ARPES, deviates significantly from band-theory calculations [2, 3, 4]. (See Fig. 7 of Ref. [4].) For energy values larger than the transfer-integrals for electron inter-chain hopping, the 1D Hubbard model is expected to provide a good description of such correlations in quasi-1D conductors [4, 13]. The model describes  $N = [N_{\uparrow} + N_{\downarrow}]$  spin-projection  $\sigma = \uparrow, \downarrow$

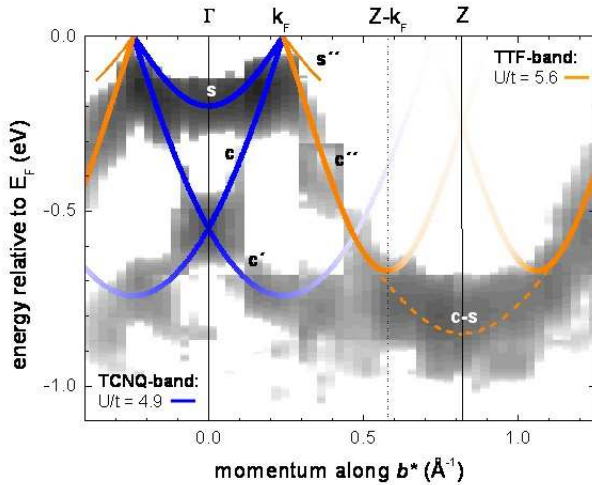


**Figure 1.** Experimental peak dispersions (grey scale) obtained by ARPES on TTF-TCNQ along the easy-transport axis as given in Fig. 7 of Ref. [4] and matching theoretical branch and border lines. (The Z-point corresponds to the momentum  $k = \pi$ .) The corresponding detailed theoretical spectral-weight distributions over the whole  $(k, \omega)$ -plane are plotted below in Fig. 2. While the theoretical charge- $c''$  and spin- $s''$  branch lines and  $c-s$  border line refer to the TTF spectral features found here ( $n = 1.41$ ,  $U/t = 5.61$ ), the charge- $c$ , spin- $s$ , and charge- $c'$  branch lines correspond to the TCNQ dispersions ( $n = 0.59$ ,  $U/t = 4.90$ ) already studied in Ref. [6].

electrons with densities  $n = N/N_a$  and  $m = [N_\uparrow - N_\downarrow]/N_a$  in an 1D lattice of  $N_a$  sites. Except in the momentum axis of Fig. 1, we use units of lattice constant one, so that  $0 \leq n \leq 2$ . We denote the electronic charge by  $-e$  and define the Fermi momentum as  $k_F = \pi n/2$  for  $n < 1$  (for electrons) and  $k_F = \pi [2 - n]/2$  for  $n > 1$  (for holes). The model includes a first-neighbor transfer-integral  $t$ , for electron hopping along the chain, and an effective on-site Coulomb repulsion  $U$ . This is one of the few realistic models for which one can exactly calculate all the energy eigenstates and their energies [14, 5]. Its low-energy spectrum belongs to the universal class of the Tomonaga and Luttinger liquid (TTL) theory [15, 16, 10]. However, its finite energy physics goes beyond (but is related to) the TTL and, until recently, it was not possible to extract from the exact solution the values of the matrix elements between the energy eigenstates. These are needed for the study of the finite-energy one-electron spectral-weight distributions. (The usual TTL theory can be considered as a special case of the finite-energy liquid used here, as we summarize below.)

Our study focuses on the theoretical description of the unusual spectral features associated with the TTF stacks, which until now has remained an open problem. The model has both spin and  $\eta$ -spin  $SU(2)$  symmetries. We denote by  $\eta$  and  $\eta_z = -[N_a - N]/2$  (and  $S$  and  $S_z = -[N_\uparrow - N_\downarrow]/2$ ) the  $\eta$ -spin value and projection (spin value and projection), respectively. For  $U/t \rightarrow \infty$  all energy eigenstates correspond

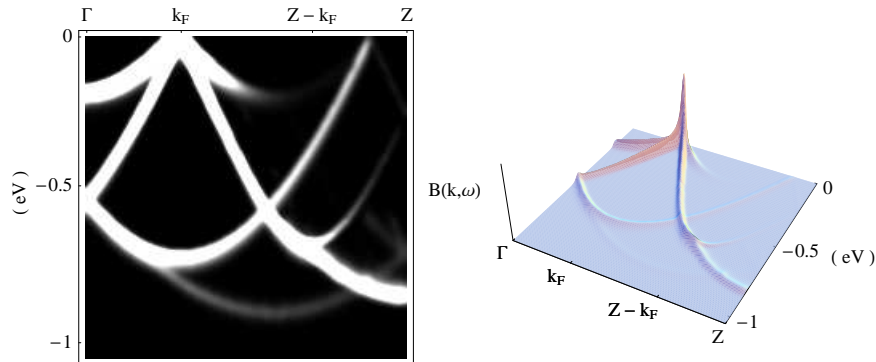


**Figure 2.** Full theoretical distribution of the one-electron removal spectral-weight intensity (left) and corresponding line shapes (right). The figures include both the TTF related spectral features for  $n = 1.41; t = 0.35 \text{ eV}; U/t = 5.61$  and those of TCNQ for  $n = 0.59; t = 0.40 \text{ eV}; U/t = 4.90$ , respectively, as in figure 1.

to electronic occupancies with fixed numbers of doubly occupied sites. However, the emergence of the exotic metallic state involves an electron - rotated-electron unitary transformation, such that rotated-electron double occupancy is a good quantum number for all  $U/t$  values [5]. As the Fermi-liquid quasiparticles, such rotated electrons have the same charge and spin as the electrons, but refer to all energies and reorganize in terms of  $[N_a - N_c]$   $\eta$ -spin  $1/2$  holons,  $N_c$  spin  $1/2$  spinons, and  $N_c$  spinless and  $\eta$ -spinless  $c$  pseudoparticles, where  $N_c$  is the number of rotated-electron singly occupied sites [5]. We use the notation  $\pm 1/2$  holons and  $\pm 1/2$  spinons, which refers to the  $\eta$ -spin and spin projections, respectively. The  $\pm 1/2$  holons of charge  $\pm 2e$  correspond to rotated-electron unoccupied (+) and doubly-occupied (-) sites. The complex behavior occurs for the  $\sigma$ -rotated electrons occupying singly occupied sites: their spin degrees of freedom originate chargeless  $\sigma$  spinons, whereas their charge part gives rise to  $\eta$ -spinless and spinless  $c$  pseudoparticles of charge  $-e$ .

Based on symmetry considerations, we can classify the  $\pm 1/2$  holons and  $\pm 1/2$  spinons into two classes: those which remain invariant under the electron - rotated-electron unitary transformation, and those which do not. The former are called independent  $\pm 1/2$  holons and independent  $\pm 1/2$  spinons, with numbers reading  $L_{c, \pm 1/2} = [\eta \mp \eta_z]$  and  $L_{s, \pm 1/2} = [S \mp S_z]$ , respectively. The latter are part of  $\eta$ -spin-zero  $2\nu$ -holon composite  $c\nu$  pseudoparticles and spin-zero  $2\nu$ -spinon composite  $s\nu$  pseudoparticles, respectively, where  $\nu = 1, 2, \dots$  is the number of  $+1/2$  and  $-1/2$  holon or  $+1/2$  and  $-1/2$  spinon pairs. The emergence of the exotic metallic state considered here involves a second unitary transformation, which maps the  $c$  pseudoparticles (and composite  $\alpha\nu$  pseudoparticles) onto  $c$  pseudofermions (and composite  $\alpha\nu$  pseudofermions) [8]. Such a transformation introduces shifts of order  $1/N_a$  in the pseudoparticle discrete momentum values and leaves all other pseudoparticle properties invariant. As a result of such momentum shifts and in contrast to the  $c$  pseudoparticles and composite  $\alpha\nu$  pseudoparticles, the corresponding pseudofermions

have no residual-interaction energy terms [8].

As discussed below, the spectral-weight distribution of TTF-TCNQ is fully determined by the occupancy configurations of the  $c$  and  $s$  pseudofermions. We denote the latter by  $s$  pseudofermions. These objects carry momentum  $q$ . For the  $m = 0$  ground-state there is  $c$  pseudofermion occupancy for  $|q| \leq 2k_F$  and unoccupancy for  $2k_F < |q| \leq \pi$ , whereas the  $s$  band is fully filled for  $|q| \leq k_F$ . (For  $m = 0$ , the exotic  $s$  band has a momentum width of  $2k_F$ .) The momentum,  $U/t$ , and  $n$  dependence of the  $\alpha = c, s$  pseudofermion energy bands  $\epsilon_\alpha(q)$ , group velocities  $v_\alpha(q) = \partial\epsilon_\alpha(q)/\partial q$ , and *Fermi-point* velocities  $v_c \equiv v_c(2k_F)$  and  $v_s \equiv v_s(k_F)$  is provided by the exact solution [5, 8]. Under the ground-state - excited-state transitions, the ground-state  $\alpha = c, s$  pseudofermions and holes are scattered by the  $\alpha' = c, s$  pseudofermions and holes created in these transitions. Such zero-momentum-forward-scattering events lead to an overall phase shift  $Q_\alpha(q)/2 = Q_\alpha^0/2 + Q_\alpha^\Phi(q, \{q'\})/2$ , where  $Q_\alpha^\Phi(q, \{q'\}) = 2 \sum_{\alpha'=c,s} \sum_{q'} \pi \Phi_{\alpha,\alpha'}(q, q') \Delta N_{\alpha'}(q')$ ,  $\pi \Phi_{\alpha,\alpha'}(q, q') = -\pi \Phi_{\alpha,\alpha'}(-q, -q')$  is a two-pseudofermion phase shift whose  $q, q', n$ , and  $U/t$  dependence is provided by the exact solution, the momentum-distribution deviation  $\Delta N_{\alpha'}(q')$  is that of the excited state, and  $Q_\alpha^0/2 = 0, \pm\pi/2$  is a scattering-less phase shift whose value is well defined for each transition. The excited-state-dependent *Fermi-point* functionals  $Q_c(\pm 2k_F)$  and  $Q_s(\pm k_F)$  fully control the spectral properties [8]. While the TLL theory involves a single interaction-dependent spectral parameter,  $1 < \xi_0 < \sqrt{2}$  [15, 16, 10], the description of the finite-energy spectral properties requires interaction and momentum-dependent phase shifts  $\pi \Phi_{c,c}(\pm 2k_F, q)$ ,  $\pi \Phi_{c,s}(\pm 2k_F, q')$ ,  $\pi \Phi_{s,c}(\pm k_F, q)$ , and  $\pi \Phi_{s,s}(\pm k_F, q')$ , where  $2k_F < |q| < \pi$  for  $n > 1$ ,  $0 < |q| < 2k_F$  for  $n < 1$ , and  $0 < |q'| < k_F$ . In the limit of low-energy, the scattering centers are created in the vicinity of the *Fermi-points* and our general description recovers the TLL theory with  $v_c(\pm 2k_F) = \pm v_c$ ,  $v_s(\pm k_F) = \pm v_s$ , and  $\xi_0 = 1 + [\Phi_{c,c}(2k_F, 2k_F) - \Phi_{c,c}(2k_F, -2k_F)] = 2[\Phi_{c,s}(2k_F, k_F) - \Phi_{c,s}(2k_F, -k_F)]$ , as further discussed in Ref. [10].

A crucial test for the suitability of the model is whether the observed ARPES peak dispersions correspond to the theoretically predicted sharpest spectral features. In figure 1 we plot the positions of the sharpest theoretical spectral features considered below but omit the corresponding detailed spectral-weight distribution over the  $(k, \omega)$ -plane predicted by the theory, which is plotted in Fig. 2. The figure also displays the experimental dispersions in the electron removal spectrum of TTF-TCNQ as measured by ARPES in Ref. [4]. Figure 2 displays specifically the full theoretical distribution of the spectral-weight intensity (left) and the line shapes (right) corresponding to the same values of  $n$  and  $U/t$  as for the theoretical lines of Fig. 1. In the evaluation of the theoretical one-electron removal spectral features plotted in Figs. 1 and 2 we apply the improved pseudofermion dynamical theory of Ref. [8]. One of our goals is to find the value of  $U/t$  for which the theoretical weight distribution leads to the best agreement with the measured TTF related ARPES spectral features.

The total number of  $\pm 1/2$  holons ( $\alpha = c$ ) and  $\pm 1/2$  spinons ( $\alpha = s$ ) reads  $M_{\alpha, \pm 1/2} = L_{\alpha, \pm 1/2} + \sum_{\nu=1}^{\infty} \nu N_{\alpha\nu}$ , where  $N_{\alpha\nu}$  denotes the number of  $\alpha\nu$  pseudoparticles.

However, for the states which control the spectral properties of TTF-TCNQ, one has that  $N_{c\nu} = 0$  for all  $\nu$  and  $N_{s\nu} = 0$  for  $\nu > 1$  and for  $n < 1$  (or  $n > 1$ ),  $N_c = N$ ,  $L_{c,+1/2} = [N_a - N]$ , and  $L_{c,-1/2} = 0$  (or  $N_c = [2N_a - N]$ ,  $L_{c,-1/2} = [N - N_a]$ , and  $L_{c,+1/2} = 0$ ) and for  $m > 0$  (or  $m < 0$ ),  $N_{s1} = N_\downarrow$ ,  $L_{s,+1/2} = [N_\uparrow - N_\downarrow]$ , and  $L_{s,-1/2} = 0$  (or  $N_{s1} = N_\uparrow$ ,  $L_{s,-1/2} = [N_\downarrow - N_\uparrow]$ , and  $L_{s,+1/2} = 0$ ). Since the independent holons and spinons of these states are scatter-less objects [8], the weight distribution is fully determined by the occupancy configurations of the  $c$  and  $s \equiv s1$  pseudofermions. For the  $(k, \omega)$ -plane regions of the ARPES data, the method used in our calculation involves specific processes associated with ground-state - excited-state transitions. For those which generate the dominant contributions one  $s$  hole is created and for densities  $n > 1$  and  $n < 1$  a  $c$  pseudofermion and a  $c$  hole, respectively, is created. The low-energy TLL corresponds to processes where both such objects are created at momentum values in the vicinity of their *Fermi points*. Since the low-energy phase of TTF-TCNQ is not metallic and corresponds to broken-symmetry states, our results are to be applied for processes with energies larger than the gap, beyond the reach of TLL theory.

For finite energy and  $U/t$  values all sharp spectral features are of power-law type, controlled by negative exponents. Important finite-energy processes are those where one  $\alpha$  pseudofermion or hole is created at  $q$  away from the *Fermi points* and the second object is created at one of these points. The preliminary studies of Ref. [6] only considered such processes. They originate features centered on lines,  $\omega = \omega_\alpha(q) = \pm\epsilon_\alpha(q)$ , in the  $(k, \omega)$ -plane. In the vicinity and just below these lines, the spectral-function reads [8, 9],

$$B(k, \omega) \approx C_\alpha(q) (\omega_\alpha(q) - \omega)^{\zeta_\alpha(q)}. \quad (1)$$

When  $\zeta_\alpha(q) < 0$ , the spectral feature is a singular branch line. The exponent reads  $\zeta_\alpha = -1 + \zeta_0(q)$ , where  $\zeta_0(q)$  is a functional whose values are fully controlled by the pseudofermion scattering. It reads,  $\zeta_0(q) = \sum_{\iota=\pm 1} \sum_{\alpha=c,s} 2\Delta_\alpha^\iota(q)$  where  $2\Delta_\alpha^\iota(q) \equiv (\iota \Delta N_{\alpha,\iota}^F + Q_\alpha^\Phi(\iota q_{F\alpha}^0, q)/2\pi)^2$ ,  $Q_\alpha^\Phi(\iota q_{F\alpha}^0, q)/2$  is the scattering part of the overall phase shift defined above,  $\iota \Delta N_{\alpha,\iota}^F = \Delta q_{F\alpha,\iota}/[2\pi/N_a]$ , and  $\Delta q_{F\alpha,\iota}$  with  $\iota = \pm 1$  is the *Fermi point* deviation relative to the ground-state values  $\iota q_{Fc}^0 = \iota 2k_F$  or  $\iota q_{Fs}^0 = \iota k_F$ . Expression (1) does not apply in the TLL regime, which corresponds to  $k \approx \pm k_F$  in Fig. 1, where the power-law exponent has a different expression [8]. The two regimes are separated by a small crossover region. Thus, the finite-energy normal state found here for TTF-TCNQ *cannot* be described by the usual TLL.

There are other important types of finite-energy processes which were not considered in the preliminary studies of Ref. [6]. Those which involve creation of more than two quantum objects lead to very little weight. In turn, some of the processes where both a  $c$  pseudofermion or hole and a  $s$  hole are created at momentum values  $q$  and  $q'$ , respectively, away from the *Fermi points* are important. When  $v_c(q) \neq v_s(q')$ , such processes do not lead to singular spectral features and generate the background spectral weight all over the  $(k, \omega)$ -plane, which although being in general small must be accounted for. (See Fig. 2.) Furthermore, a second type of sharp feature not considered in Ref. [6] corresponds to lines generated by such processes when both created objects

move with the same group velocity,  $v_c(q) = v_s(q')$ , and the spectral feature corresponds to a border line,  $\omega = \omega_{BL}(k) = [\pm\epsilon_c(q) - \epsilon_s(q')] \delta_{v_c(q), v_s(q')}$ , in the  $(k, \omega)$ -plane. The spectral function reads [9],

$$B(k, \omega) \approx C_{BL}(k) (\omega - \omega_{BL}(k))^{-1/2}, \quad (2)$$

in the vicinity and just above such a line. The TTF line called  $c - s$  in Fig. 1 and the weaker TCNQ bottom line of Fig. 2 are of this type. The latter weaker theoretical line is not plotted in Fig. 1, yet it clearly marks the lower limit of the experimental weight distribution. In the limit of  $U/t \gg 1$ , our one-electron weight distributions agree with those of Ref. [17].

By careful analysis of the  $k$ ,  $\omega$ , and  $U/t$  dependence of the obtained theoretical weight distribution, we find that for  $n = 1.41$  the electron removal spectrum calculated for  $t = 0.35$  eV and  $U = 1.96$  eV ( $U/t = 5.61$ ) yields the best agreement with the TTF experimental dispersions. (The  $U/t = 5.61$  TTF value is much larger than that preliminarily estimated in Ref. [6].) Remarkably, the only fitting parameter is  $U/t$ . For the considered values of  $n$  and  $U/t$ , the singular charge- $c''$  and spin- $s''$  branch lines and the singular  $c - s$  border line of Fig. 1 correspond to the sharp spectral features of the model one-electron removal spectral function for the ARPES  $(k, \omega)$ -plane region. The fading parts of the theoretical charge- $\alpha = c', c''$  branch lines of Fig. 1, not seen in the experiment, correspond to values of the momentum where the constant  $C_\alpha(q)$  of the expression (1) in the vicinity of these lines is small. Although there is a reasonably good overall quantitative agreement between the theoretical one-electron weight distributions and the TTF related features measured by ARPES, there are apparent differences in the finest details, for instance the broadening of some of the sharp features predicted by the theory. However and in spite of the recent improvements in the resolution of photoemission experiments [2, 3, 4], it is difficult to measure the weight-distribution finest details experimentally, in part due to the extrinsic losses that occur on anisotropic conducting solids [18]. Hence while our theoretical description provides the dominant microscopic processes behind the overall unusual spectral-weight distribution observed in the real material, it is difficult to judge which other smaller effects may play some role in the weight-distribution finest details.

Our general study refers to the whole  $(k, \omega)$ -plane and confirms the validity of the predictions of Ref. [6] for the TCNQ related spectral features: for  $n = 0.59$  the finite-energy-electron-removal spectrum calculated for  $t = 0.40$  eV and  $U = 1.96$  eV ( $U/t = 4.90$ ) yields an almost perfect agreement with the TCNQ experimental dispersions, which correspond to the spin- $s$ , charge- $c$ , and charge- $c'$  branch lines of Fig. 1 and the weaker border line shown in Fig. 2. There we plot the full theoretical distribution of the weight intensity resulting from electron removal both for  $n = 1.41; U/t = 5.61$  and  $n = 0.59; U/t = 4.90$  and the corresponding line shapes, respectively.

Our results reveal that the ARPES peaks refer to separate spin ( $s$  hole) and charge ( $c$  pseudofermion or hole) objects for the whole energy bandwidth, whose line-shape depends on the interaction. For the Hubbard model, such a spin-charge separation

persists in the limit of low energy, where the quantum liquid becomes a TLL. An important exception is the TTF singular border line named  $c - s$  in Fig. 1 (and the weaker TCNQ border line shown in Fig. 2), which refers to a charge and a spin object moving with the same velocity. Before merging this line, the charge- $c''$  branch line refers to  $q$  values such that  $|v_c(q)| > v_s$ , whilst for  $q$  and  $q'$  obeying the relation  $v_c(q) = v_s(q')$  such that  $0 \leq |v_c(q)| = |v_s(q')| \leq v_s$  the singular  $c - s$  border line emerges. Such a feature does not exist at low energy because of differing charge and spin velocities.

The transfer-integral values obtained here are about twice as large as those found by band theory, consistently with the experimental bandwidth being much larger than predicted by traditional estimates [2]. Moreover, our values for  $U/4t$  are of the order of unity and larger for TTF ( $U/t = 5.61$ ) than for TCNQ ( $U/t = 4.90$ ), consistently with the TTF-TCNQ broken-symmetry-states and optical properties [1]. The effects of the onsite repulsion  $U$  considered here for the electrons inside the solid, lead to a weight distribution that agrees with the general ARPES spectrum structure over a wide range of finite energies. (This is in contrast to band-theory calculations, as confirmed in Fig. 7 of Ref. [4].) However, when the photoelectron is in the vacuum above the crystal it may create excitations in the substrate via long-ranged interactions beyond our model. The resulting inelastic losses as well other effects of finite temperature and long-range Coulomb interactions [19] are expected to be the mechanisms behind the broadening of the singular features predicted here [18]. Such effects lead to the broad peaks observed in the ARPES of Ref. [4] but do not change their overall distribution over the  $(k, \omega)$  plane, which remains as found in this paper.

We thank R. Claessen, N. M. R. Peres, T. C. Ribeiro, and M. Sing for discussions and the support of ESF Science Program INSTANS, European Union Contract 12881 (NEST), FCT grants SFRH/BD/6930/2001, POCTI/FIS/58133/2004, and PTDC/FIS/64926/2006 and OTKA grant T049607.

- [1] Basista H, Bonn D A, Timusk T, Voit, Jérôme D and Bechgaard K 1990 *Phys. Rev. B***42** 4088.
- [2] Zwick F, Jérôme D, Margaritondo G, Onellion M, Voit J and Grioni M 1998 *Phys. Rev. Lett.***81** 2974.
- [3] Claessen R, Sing M, Schwingenschlögl U, Blaha P, Dressel M and Jacobsen CS 2002 *Phys. Rev. Lett.* **88** 096402.
- [4] Sing M, Schwingenschlögl U, Claessen R, Blaha P, Carmelo JMP, Martelo LM, Sacramento PD, Dressel M and Jacobsen CS 2003 *Phys. Rev. B***68** 125111.
- [5] Carmelo JMP, Román JM and Penc K 2004 *Nucl. Phys. B***683** 387.
- [6] Carmelo JMP, Penc K, Martelo LM, Sacramento PD, Lopes dos Santos JMB, Claessen R, Sing M and Schwingenschlögl U 2004 *Europhys. Lett.***67** 233.
- [7] Carmelo JMP, Penc K, Sacramento PD, Sing M and Claessen R 2006 *J. Phys.: Cond. Mat.***18** 5191.
- [8] Carmelo JMP, Penc K and Bozi D 2005 *Nucl. Phys. B***725** 421; 2006 *Nucl. Phys. B (erratum)***737** 351; Carmelo JMP and Penc K 2006 *Eur. Phys. J. B***51** 477. Carmelo JMP and Penc K 2006 *J. Phys.: Cond. Mat.***18** 2881.
- [9] Carmelo JMP and Bozi D 2007, submitted to *Annals of Physics*.
- [10] Carmelo JMP, Martelo LM and Penc K 2006 *Nucl. Phys. B***737** 237; Carmelo JMP and Penc K 2006 *Phys. Rev. B***73** 113112.
- [11] Benthien H, Gebhard F and Jeckelmann E 2004 *Phys. Rev. Lett.***92** 256401.
- [12] The reason for such a discrepancy is that the present method takes into account all spectral features

distributed over the whole  $(k, \omega)$ -plane, whereas the analysis of Ref. [6] relied on the momentum and energy dependence in the vicinity of the branch lines only.

- [13] Vescoli V, Degiorgi L, Henderson W, Grüner C, Starkey KP and Montgomery LK 1998 *Science***281** 181.
- [14] Lieb Elliot H and Wu FY 1968 *Phys. Rev. Lett.***20** 1445; Martins MJ and Ramos PB 1998 *Nucl. Phys. B***522** 413.
- [15] Schulz HJ 1990 *Phys. Rev. Lett.***64** 2831.
- [16] Voit J 1995 *Rep. Prog. Phys.***58** 977.
- [17] Penc K, Hallberg K, Mila F and Shiba H 1996 *Phys. Rev. Lett.***77** 1390.
- [18] Joynt R 1999 *Science***284** 777; Mills DL 2000 *Phys. Rev. B***62** 11197; Joynt R 2002 *Phys. Rev. B***65** 077403.
- [19] Abendschein A and Assaad FF 2006 *Phys. Rev. B***73** 165119; Bulut N, Matsueda H, Tohyama T and Maekawa S 2006 *Phys. Rev. B***74** 113106.